Applications of RO Data in Space Weather

User Preparation Webinar on EPS-SG Radio Occultation Mission

28th October, 2021

Riccardo Notarpietro, EUMETSAT

Manuel Hernandez Pajares, Universitat Politècnica de Catalunya

Outlook

- Radio Occultation and Ionosphere / Space Weather monitoring
- Overview on the GRAS ionospheric extension experiment on EPS Metop-A
- Ionospheric monitoring capabilities of the RO instrument on EPS-SG and products description
- Electron density profile retrieval: extension to EPS-SG satellites orbit. Advancements and recent results

EUMETSAT

Radio Occultation for Ionosphere and Space Weather

- The Radio Occultation (RO) Global Navigation Satellite Systems (GNSS) measurements are typically gathered from a Low Earth Orbiting receiver with line-of-sights below its local horizon. They are thus very sensitive to the vertical variation of the atmospheric refractivity in the occultation region: mostly neutral / ionospheric below / above ~70 km.
- As a consequence, the RO GNSS measurements are crucial to get vertical profiles, from the ground to the LEO height, of ionospheric scintillation indices and electron density and, in general, to be able to perform realistic high resolution ionospheric tomography and data assimilation, also in the rapidly changing Space Weather scenario.

EUMETSAT

RO and Ionosphere / Space Weather monitoring

N. Jakowski et al., **Space weather monitoring by GPS measurements on board CHAMP**, *Space Weather*, 2007

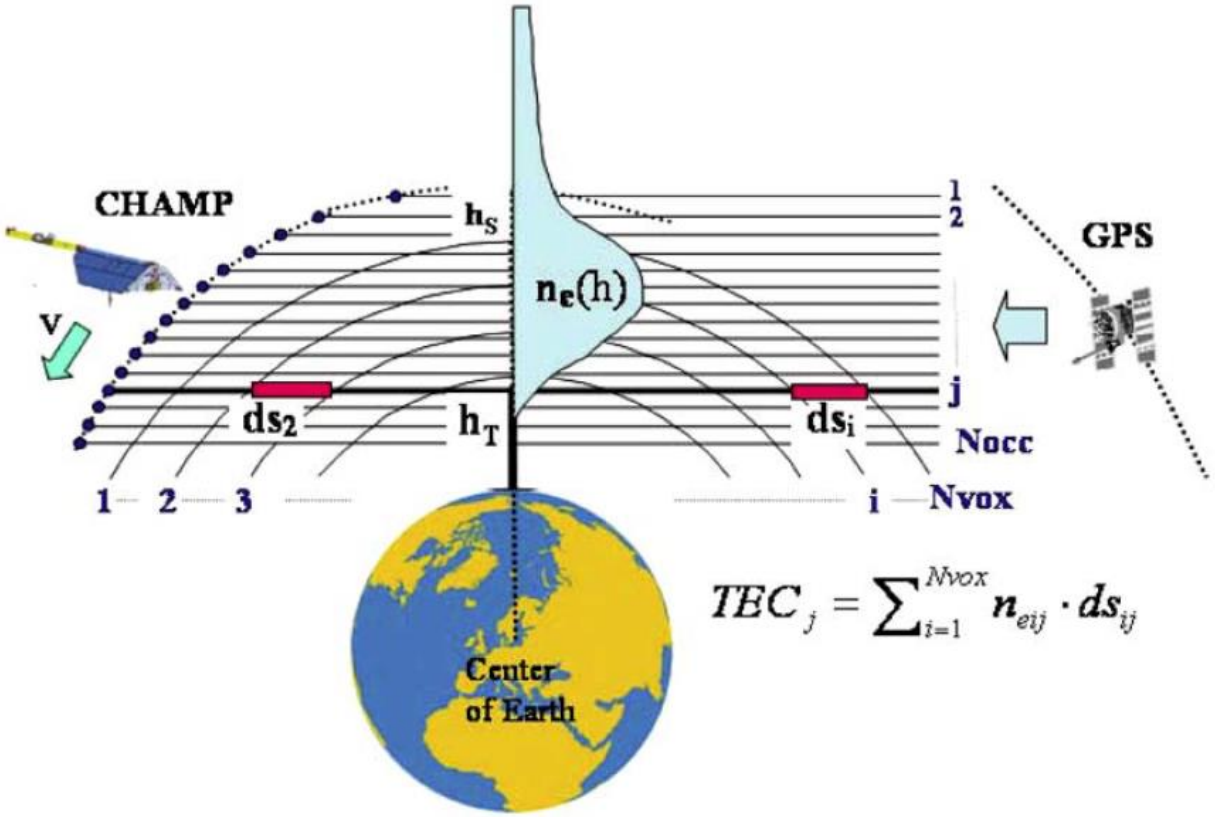

Figure 2. Principle of GPS radio occultation measurements and data inversion.

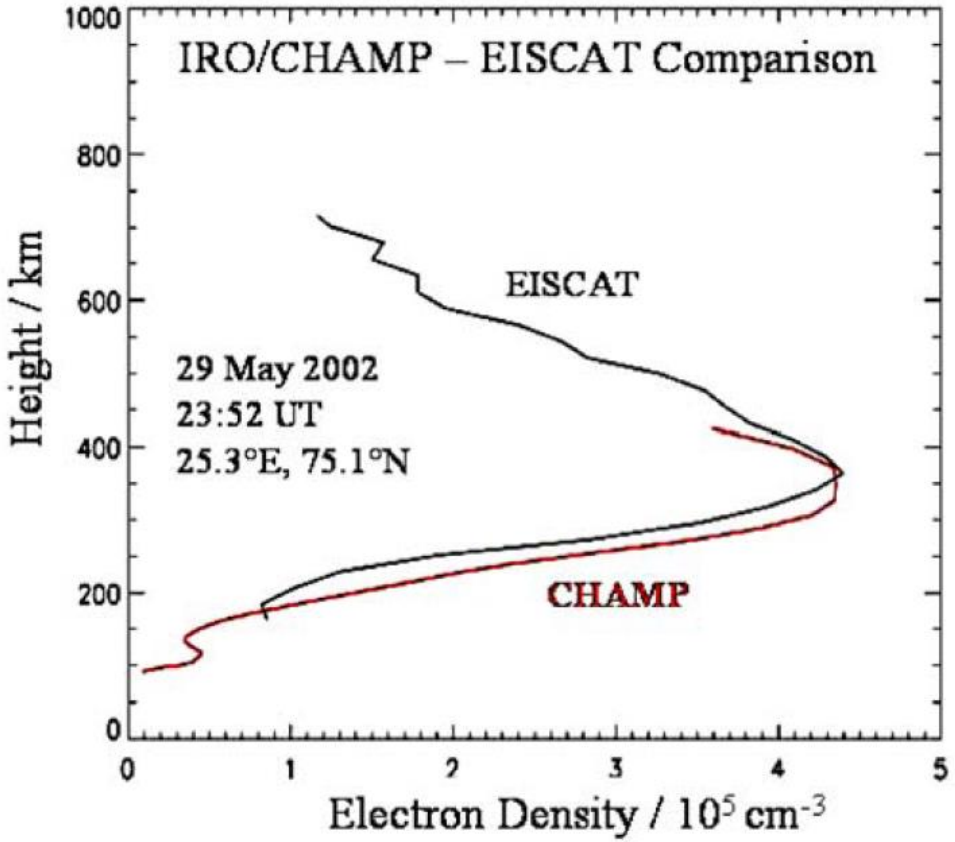

Figure 5. Comparison of an electron density profile derived from CHAMP data with corresponding EISCAT data measured on 29 May 2002 [*Stolle et al.*, 2004].

EUMETSAT

Higher vertical resolution taking into account horizontal gradients: Improved Abel transform

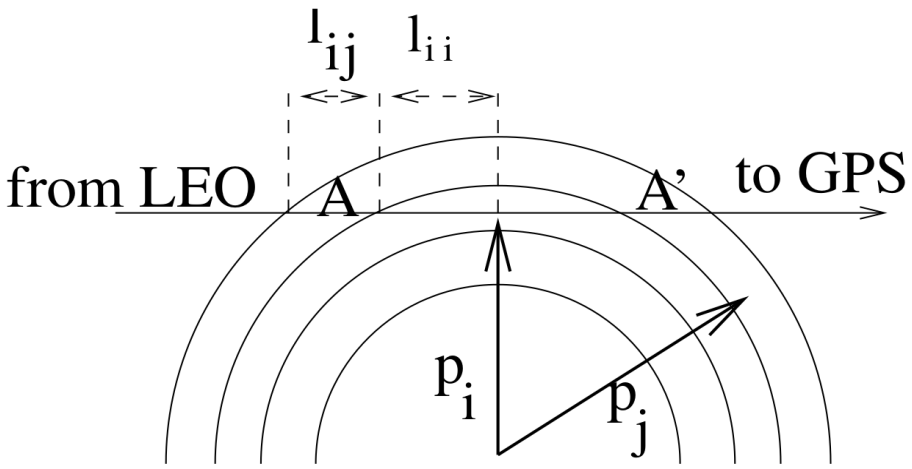

Figure 1. Layout of the inversion model geometry.

Starting from the outer ray ($p_1 = r_{LEO}$) , for a given ray i, where $i = 1...$, with impact parameter, p_i, its $STEC$ can be written in a discrete representation as (see Figure 1):

$$STEC(p_i) = \quad 2 \cdot l_{ii} \cdot TEC(LT_{ii}, \Phi_{ii}) \cdot F(p_i) + \sum_{j=1}^{j=i-1} l_{ij} \left[TEC(LT_{ij}, \Phi_{ij}) + TEC(LT'_{ij}, \Phi'_{ij}) \right] F(p_j) \tag{4}$$

where LT_{ij}, LT'_{ij}, Φ_{ij} and Φ'_{ij} are the horizontal coordinates of the two intersection points between the ray i and the layer j.

Table 1. Fractional differences between ionosonde frequencies and occultation derived frequencies. In each column the first sub-column corresponds to the separability hypothesis and the second sub-column to the spherical symmetry hypothesis.

	Internal comparisons		foF2 all LT		foF2 no dawn occ.		foF2 dawn occ.		foE	
	Sep.	Sph.	Sep.	Sph.	Sep.	Sph.	Sep.	Sph.	Sep.	Sph.
# comparisons	30	30	114	114	90	90	24	24	16	16
mean (%)	-0.9	-3.8	1.6	0.3	0.0	-1.8	7.8	8.3	-4.2	-14.8
rms (%)	11.0	22.2	8.8	14.1	6.9	11.2	13.6	21.5	15.0	21.0

Hernández-Pajares et al, **Improving the Abel inversion by adding ground GPS data to LEO radio occultations in ionospheric sounding,** *GRL*, 2000.

EUMETSAT

RO and Ionosphere / Space Weather monitoring: Scintillations

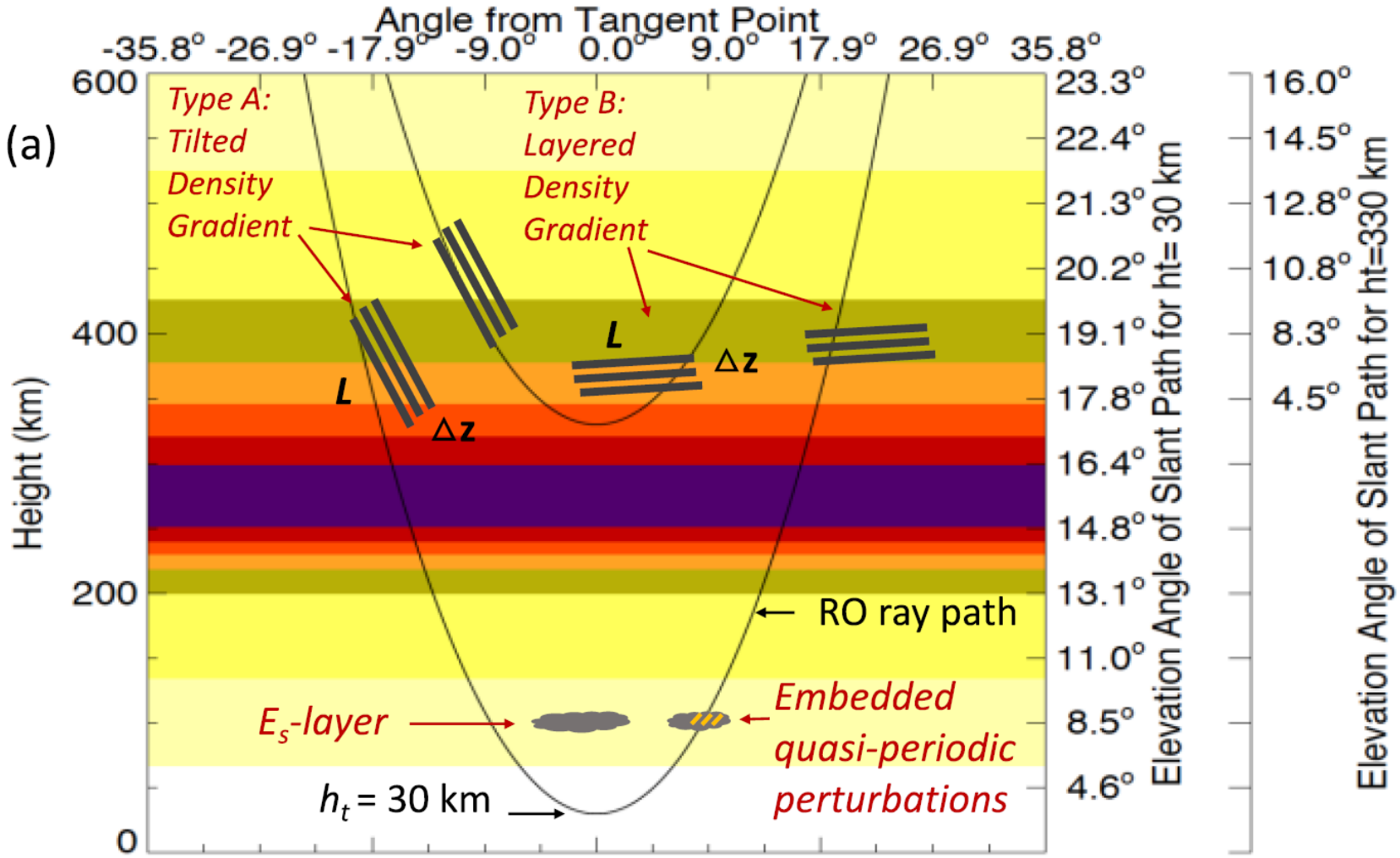

Slant view geometry for the GNSS RO observations at ht = 30 km and ht = 330 km

Dong Wu, **Ionospheric S4 Scintillations from GNSS Radio Occultation (RO) at Slant Path**, *Remote Sensing*, 2020.

Depending on the tilt angle of structured ionospheric disturbances, their impacts on the observed scintillation amplitude may be different.

Scintillations from a deep slant view are more sensitive to the tilted than layered density gradients.

EUMETSAT

RO and Ionosphere / Space Weather monitoring: Scintillations

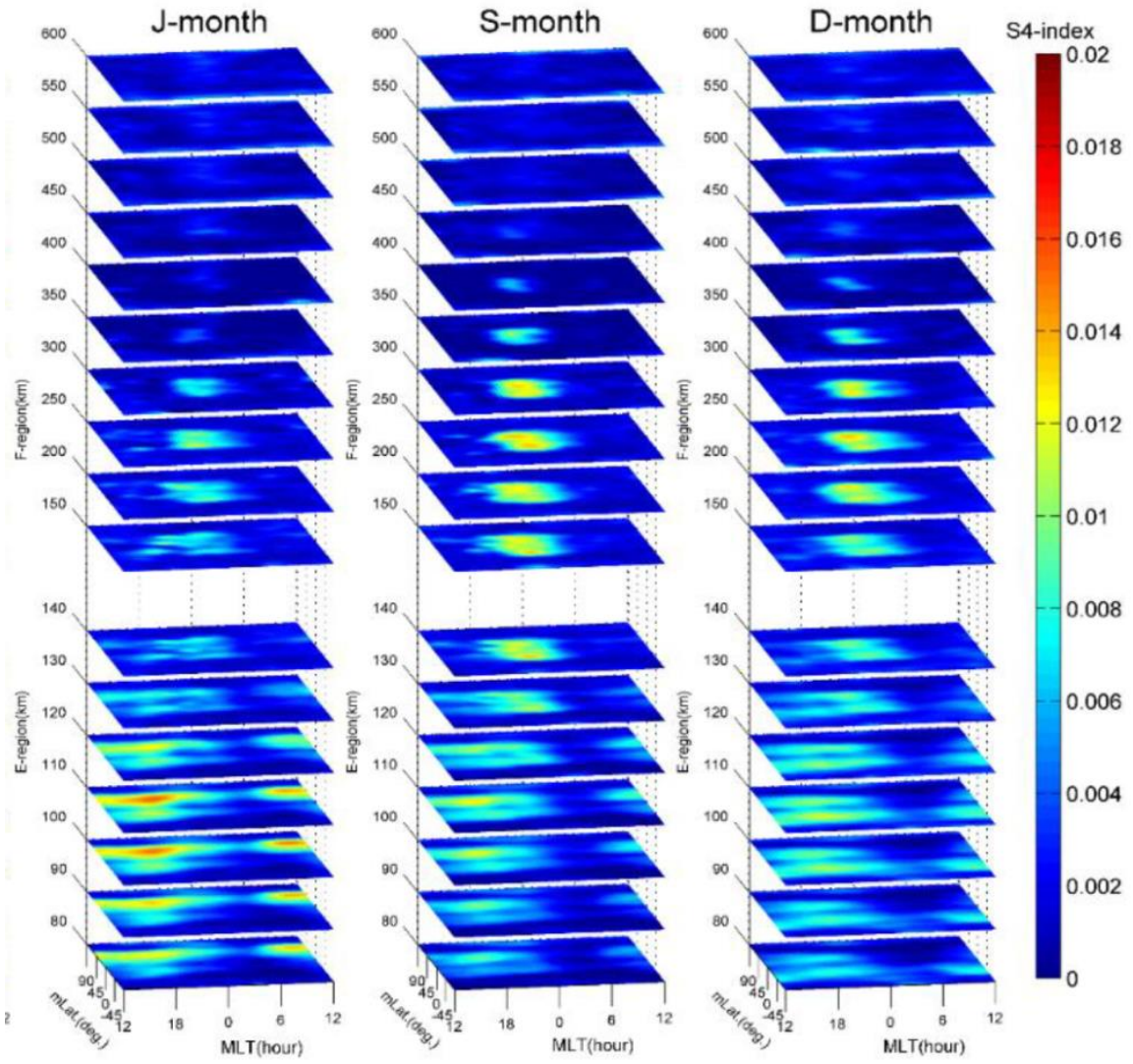

June, September and December (left to right) S4max scintillation indices from COSMIC during low solar activity in 2008

Liu et al., **Worst-Case GPS Scintillations on the Ground Estimated from Radio Occultation Observations of FORMOSAT-3/COSMIC During 2007–2014**, *Surv. Geophys.*, 2016.

RO and Ionosphere / Space Weather monitoring: Sporadic E-layer monitoring

Arras C. et al., **A global climatology of ionospheric irregularities derived from GPS radio occultation**, *GRL*, 2008.

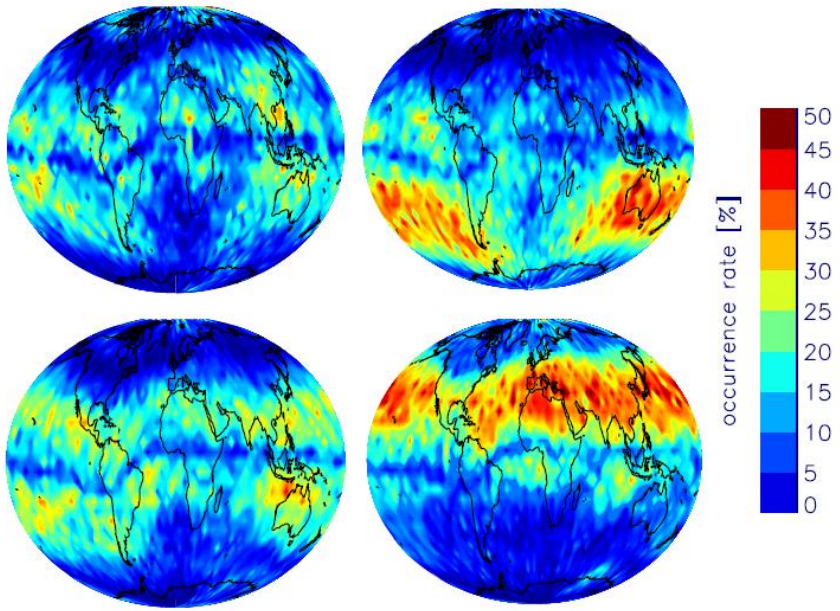

Figure 3. Seasonal occurrence of E_s detected with CHAMP, GRACE and FORMOSAT-3/COSMIC with a resolution of 5° × 5°. Plots for the (top left) autumn (September, October, November) 2006 and (top right) winter (December, January, February) 2006/2007. Data from (bottom left) spring (March, April, May) 2007 and (bottom right) summer (June, July, August) 2007.

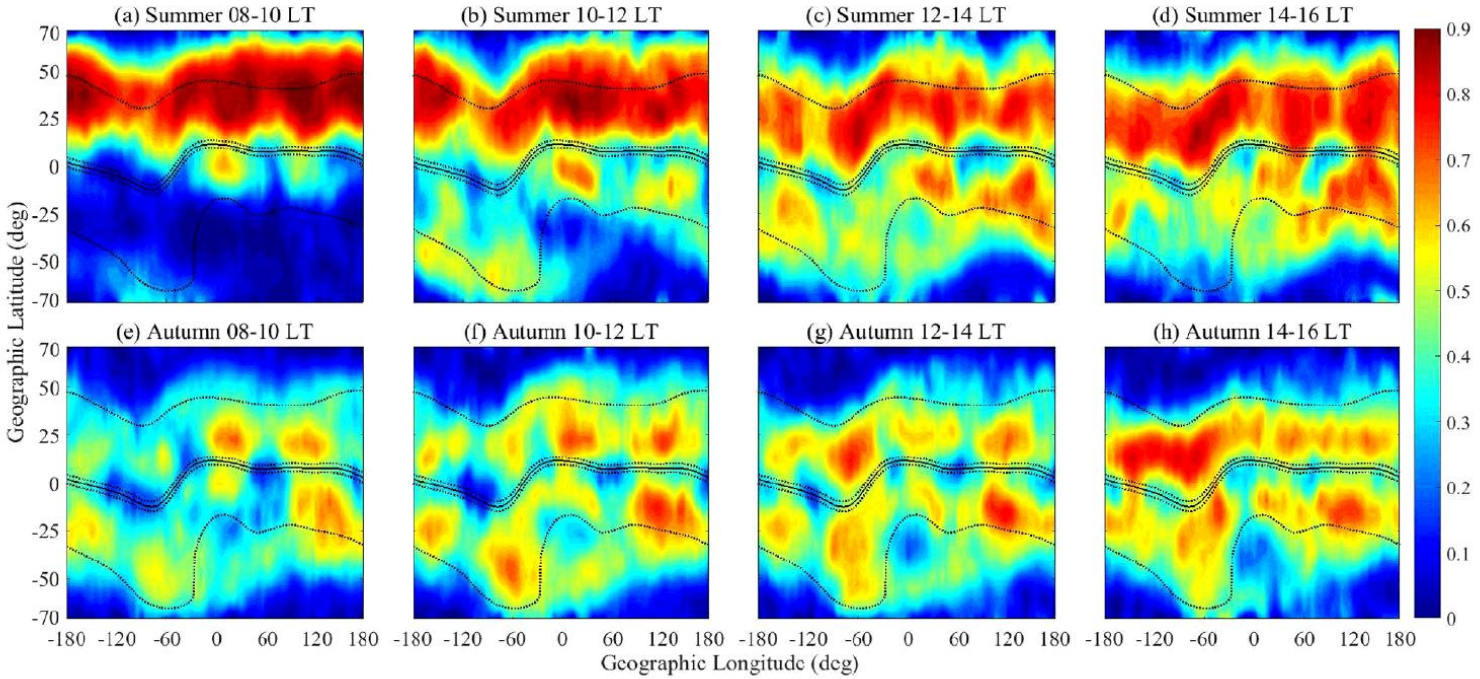

Figure 3. Global distributions of the Es occurrence rate at altitudes ranging between 105 and 115 km in the boreal summer (top row) and autumn (bottom row).

Liu Z et al., **Wavenumber-4 Patterns of the Sporadic E Over the Middle- and Low-Latitudes**, *JGR Space Physics*, 2021

EUMETSAT

First ionospheric tomography with GNSS ROs under SW

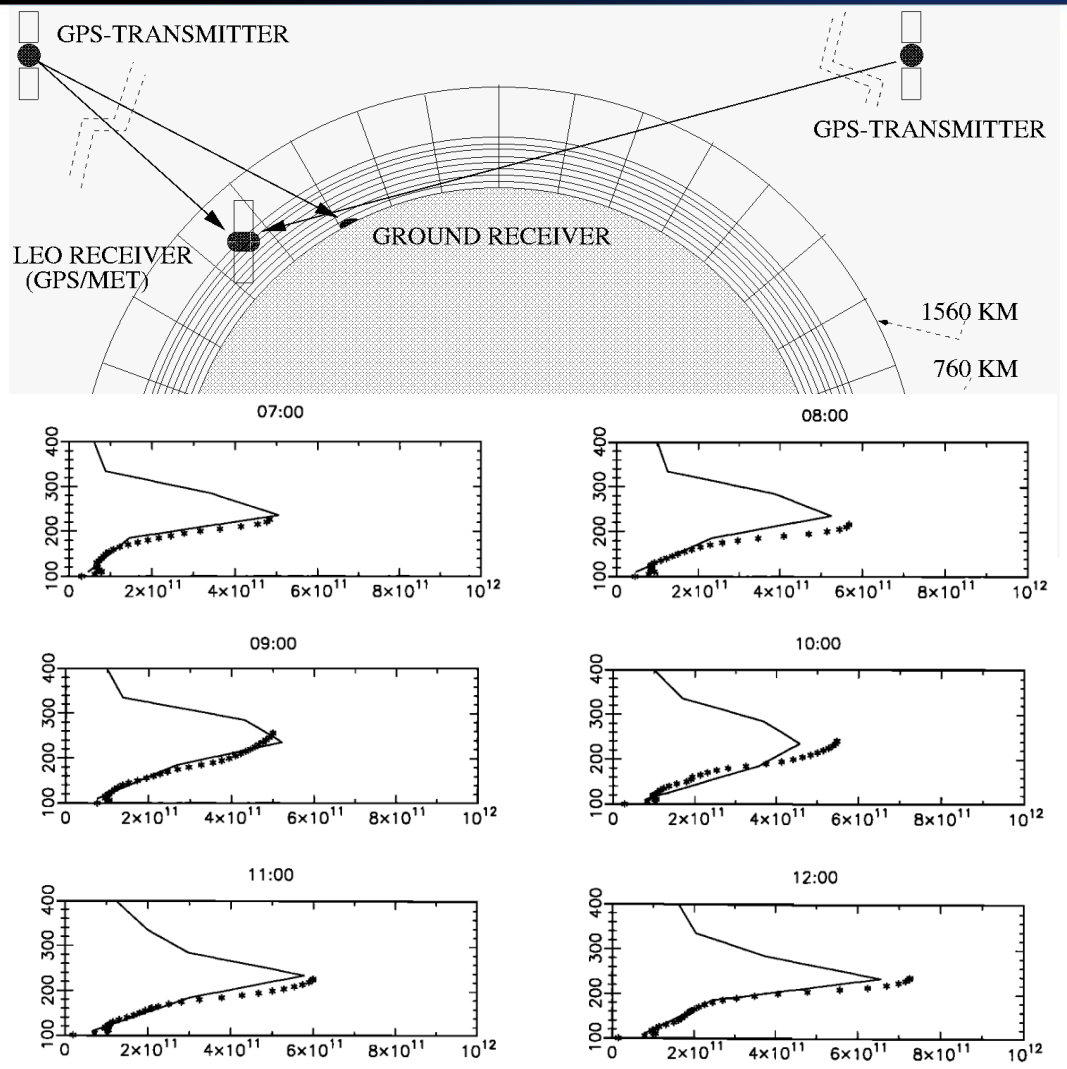

Figure 5. Comparison of the bottomside electron density profiles between Ebre observatory ionosonde and our results for October 18, 1995. The vertical axis contains the electron density ranging from 0 to 10^{12} electrons/m^3 and the vertical axis the height between 100 to 400 km. Each label indicates the UT that approximately corresponds with the local time at Ebre Observatory (0.5 deg of longitude).

These figures correspond to the ionospheric tomography performed combining COSMIC RO and POD GPS measurements with ground-based GPS measurements, during two geomagnetic storms, summarized in

Hernández-Pajares et al. **Global observation of the ionospheric electronic response to solar events using ground and LEO GPS data**. *JGR-SP*, 1998

which was the first usage of GNSS radio occultations for Space Weather studies, following the review paper

Bust & Mitchell, **History, current state, and future directions of ionospheric imaging**, 2008.

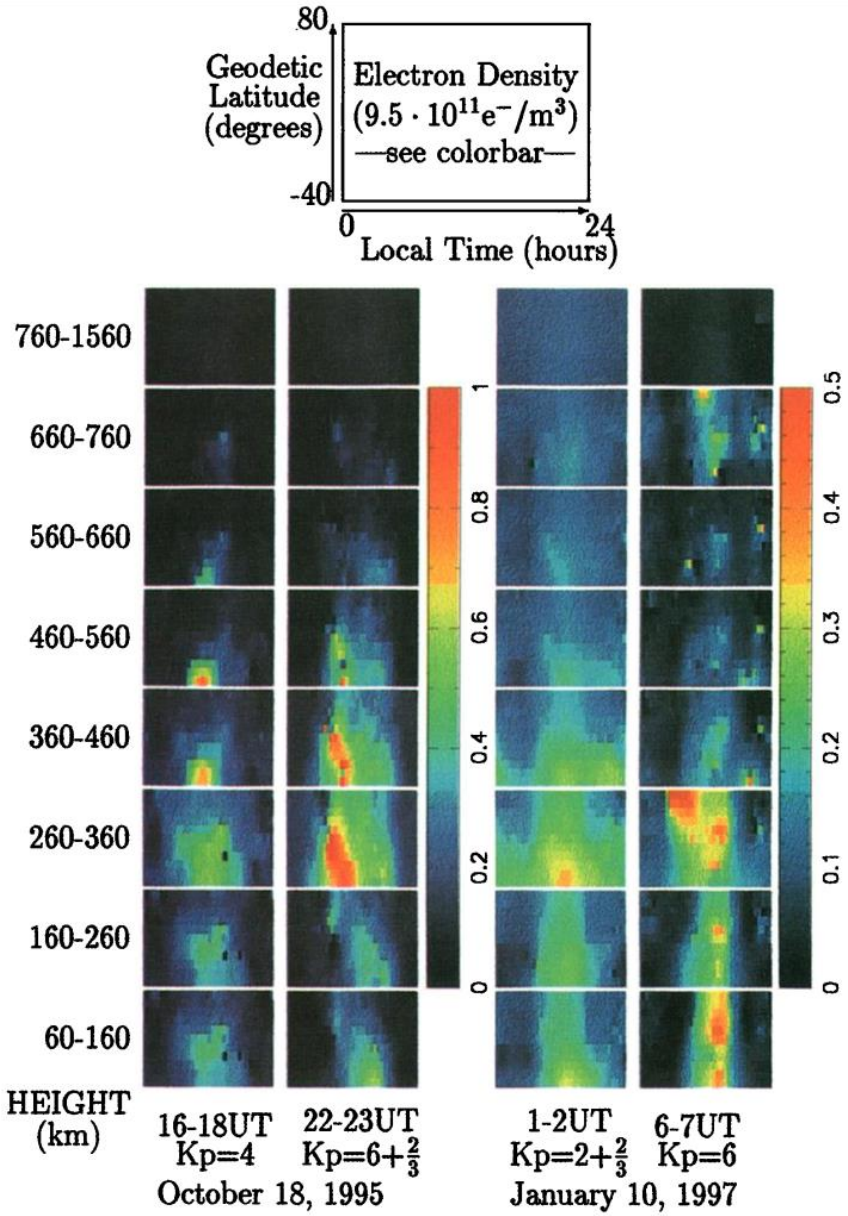

Topside Ionosphere and Plasmasphere Modelling Using GNSS Radio Occultation and POD Data

NmF2 (10^{12} el/m3), hmF2 (km) and topside VTEC (10^{16} el/m2) zonal means obtained by

- assimilating sTEC estimated by the POD COSMIC data
- using Ne(h) derived by RO measurements performed by COSMIC satellites as background.

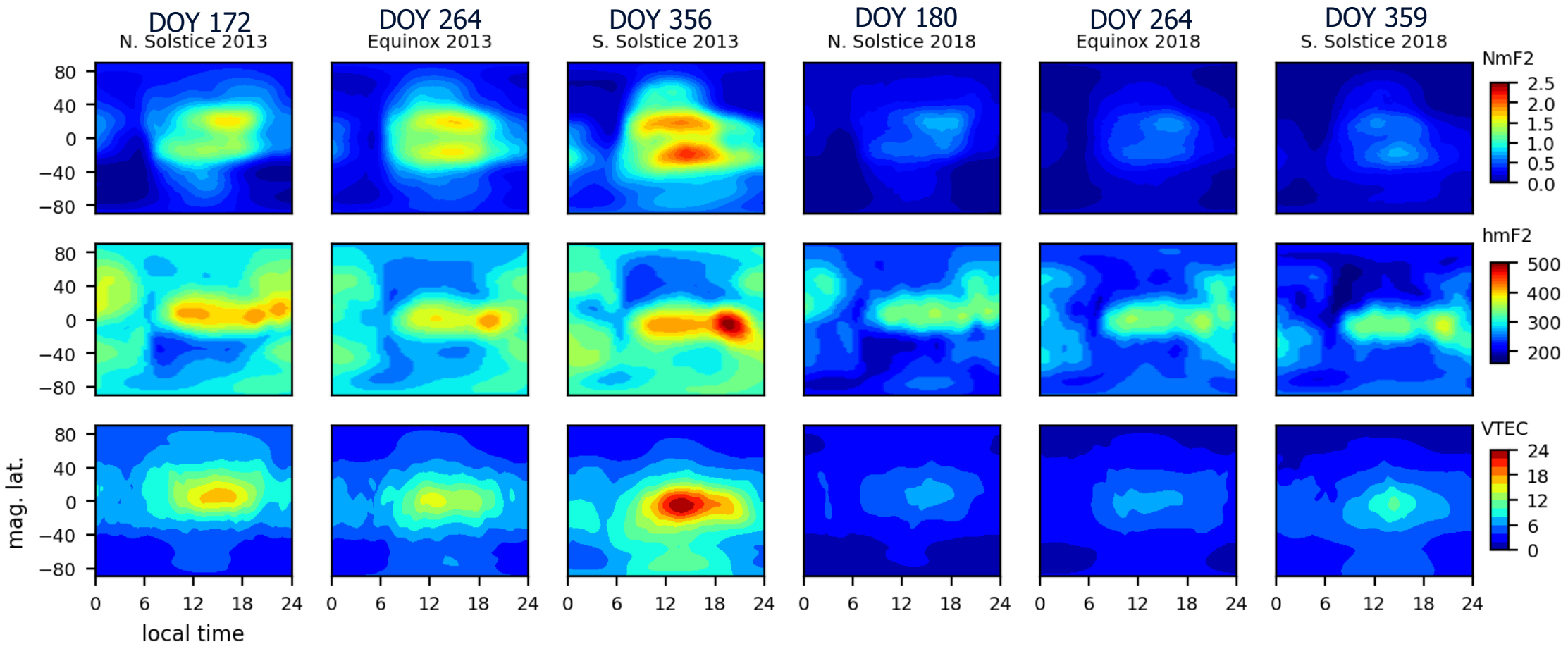

Prol, F.S.; Hoque, M.M, **Topside Ionosphere and Plasmasphere Modelling Using GNSS Radio Occultation and POD Data**, *Remote Sens*, 2021

EUMETSAT

Overview on the GRAS ionospheric extension experiment on EPS Metop-A

GRAS on Metop-A ionospheric extension experiment

- **Metop/GRAS** measurements go up to 80 km, only covering the neutral atmosphere.

- During the Metop-A end-of-life technology test campaign in 2020, we temporarily extended the vertical measurement range of GRAS into the lower ionosphere:
  - Up to 300 km altitude as candidate for a future operational implementation
  - Up to 600 km to gather science data

		SLTA coverage [km]
23/06 ÷ 14/07	~ 3 weeks	-250/300
15/07 ÷ 26/08	~ 6 weeks	-200/600
27/08 ÷ 09/09	~ 2 weeks	-300/300

- Despite expected limitations (antenna gain / number of channels available) we have demonstrated that we can provide
  - dual frequency, high rate Bending Angles
  - dual frequency, high rate ionospheric Scintillation Indexes (S_4/σ_φ)

from GRAS without impacting neutral atmospheric occultation data provision to our users

EUMETSAT

Ionospheric SNR and bending angles

L1 and L2 SNR profiles

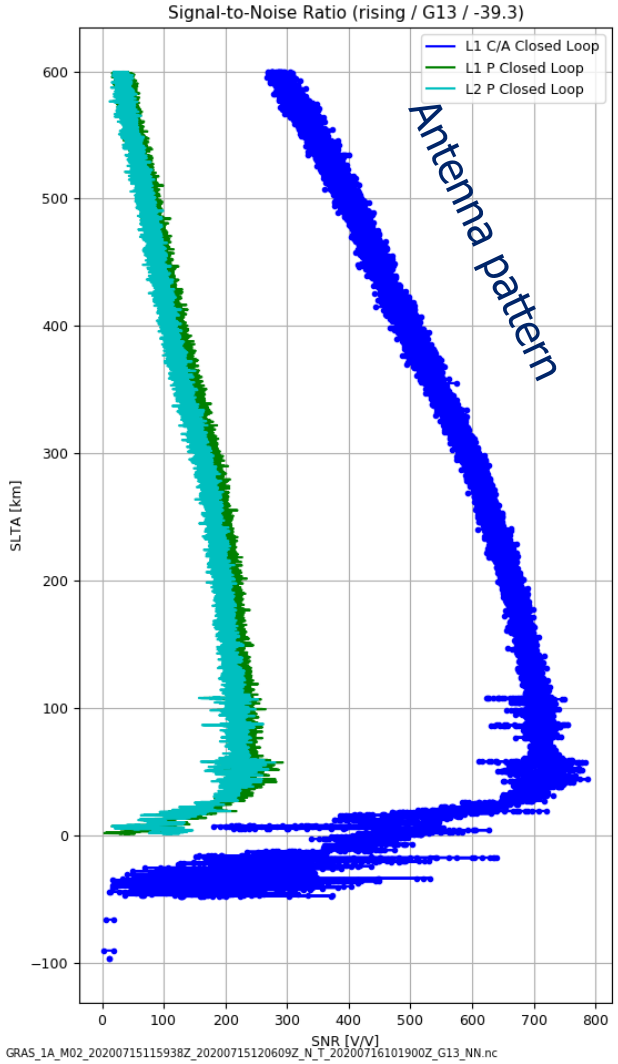

- Note the decrease of SNR above ~100 km due to the antenna gain patterns.

EUMETSAT

Ionospheric SNR and bending angles

L1 and L2 SNR profiles

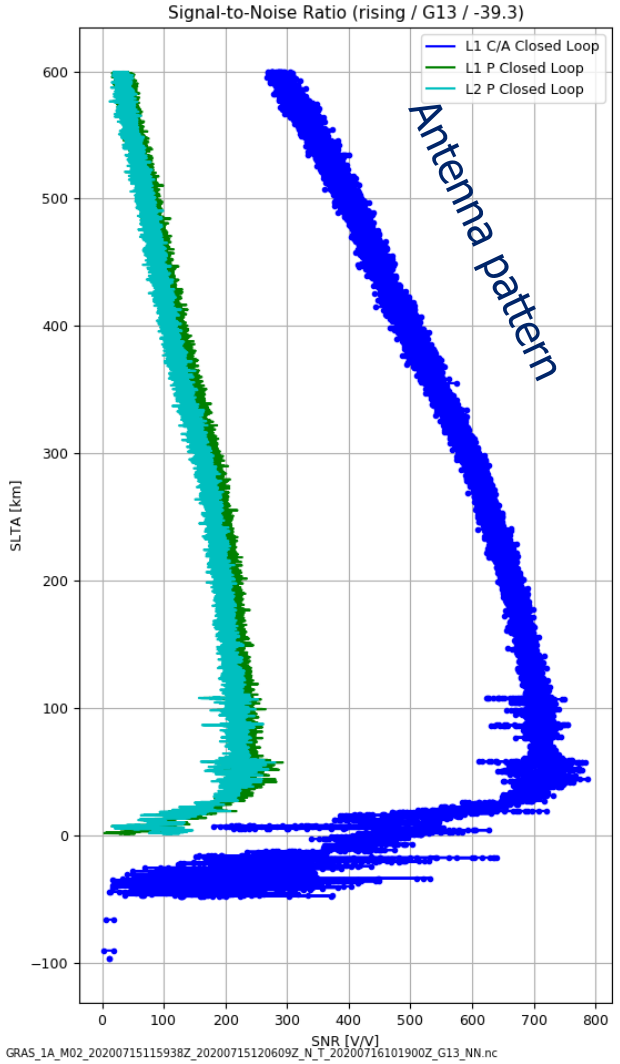

- Note the decrease of SNR above ~100 km due to the antenna gain patterns.
- In almost all cases, dual-frequency bending angles can be retrieved even up to 600 km.

L1 and L2 Bending angle profiles

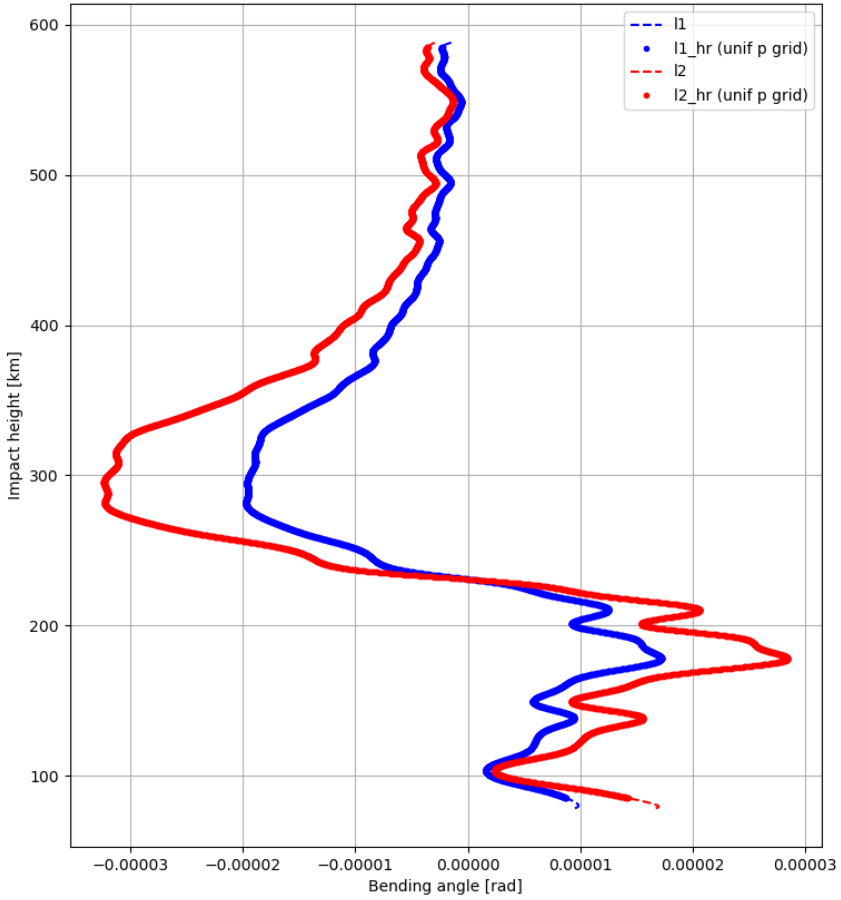

EUMETSAT

Ionospheric SNR and bending angles

L1 and L2 SNR profiles

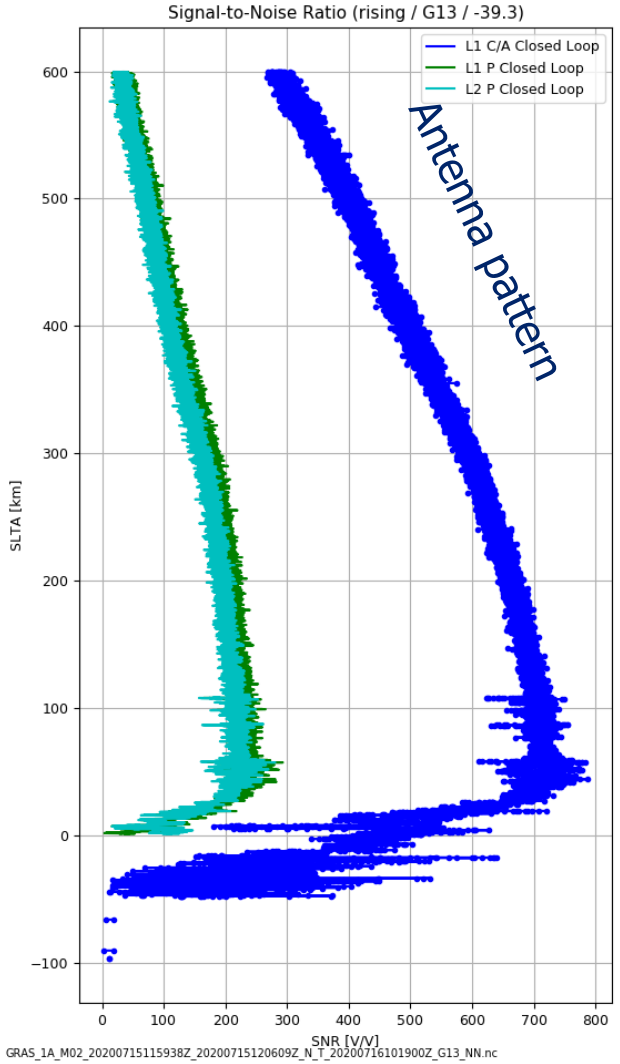

- Note the decrease of SNR above ~100 km due to the antenna gain patterns.
- In almost all cases, dual-frequency bending angles can be retrieved even up to 600 km.

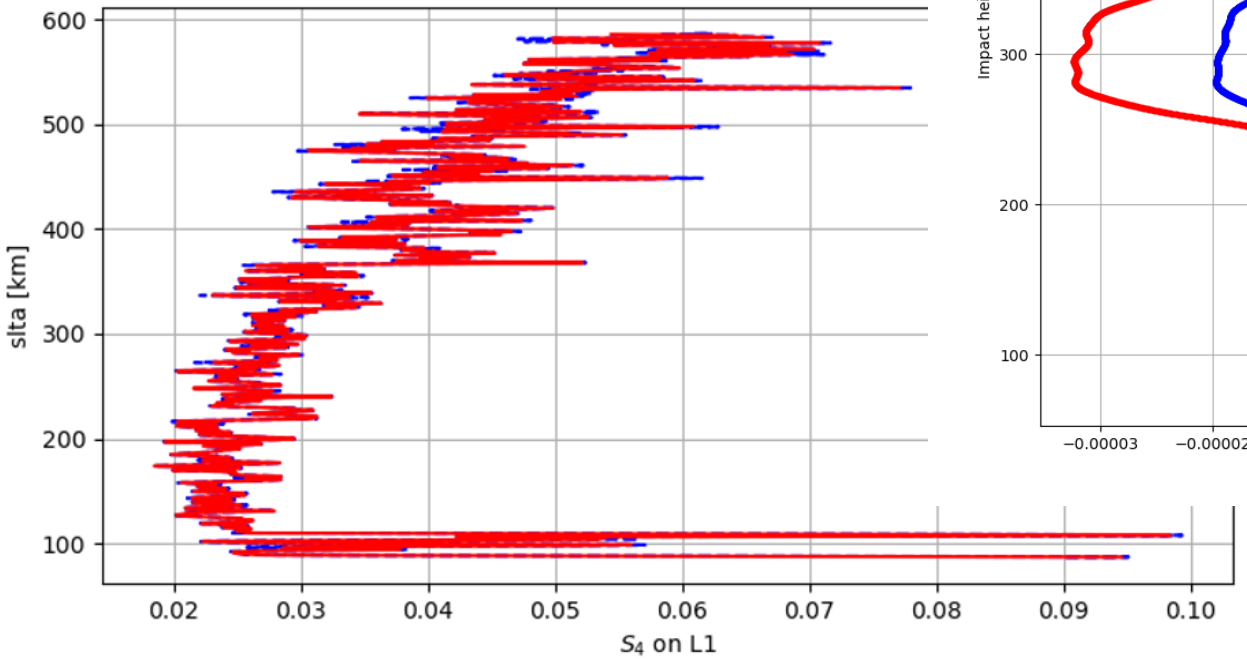

L1 and L2 Bending angle profiles

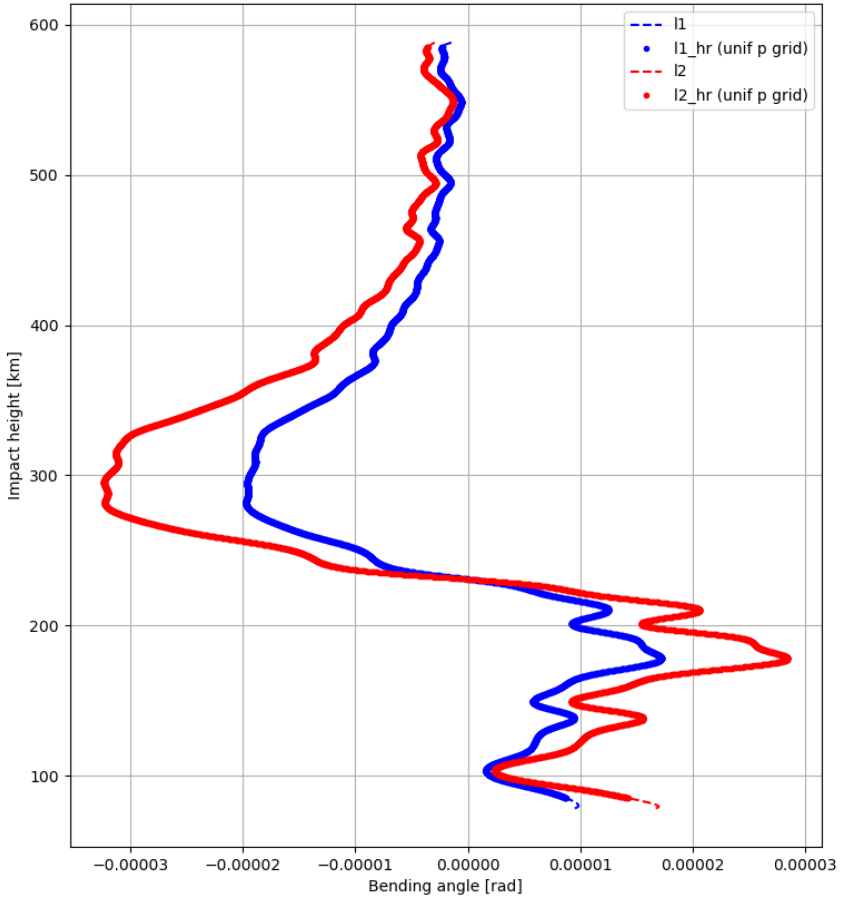

EUMETSAT

Scintillations (Es-layer) zonal mean (S4 on L1 signal)

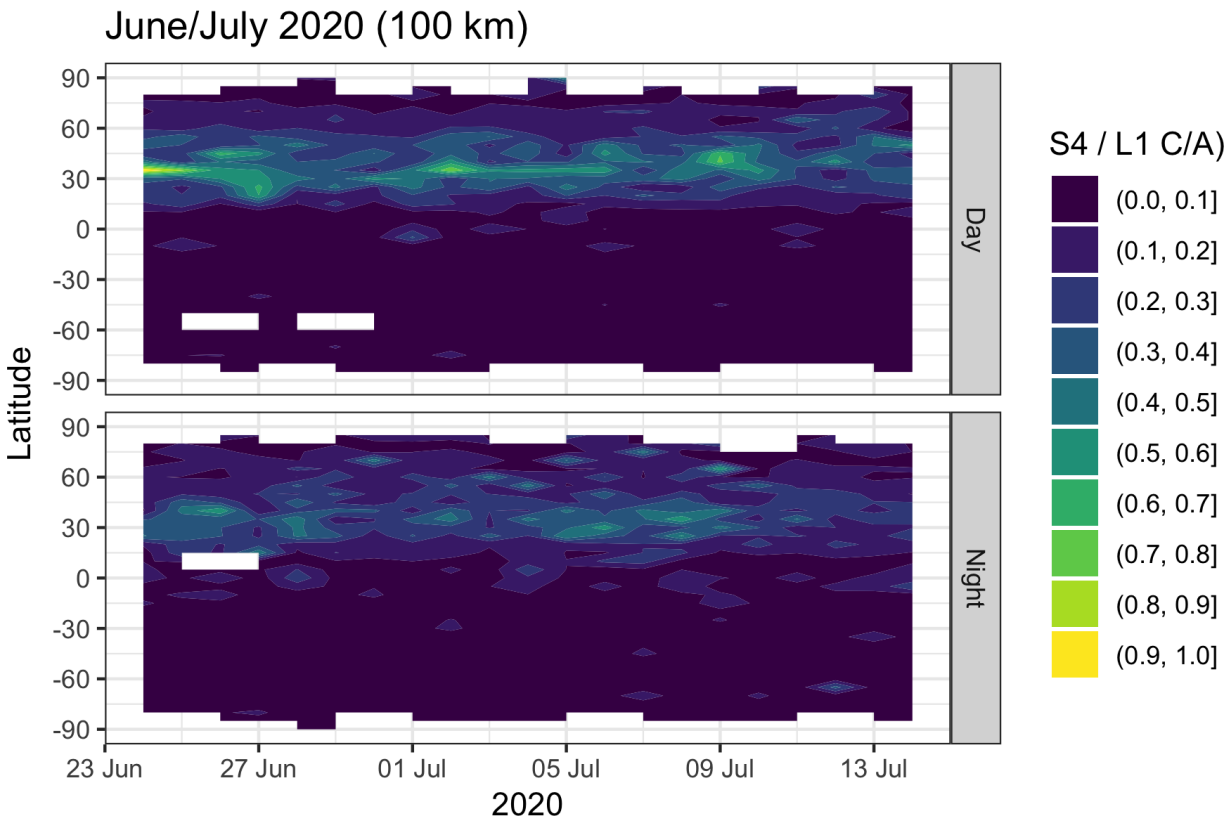

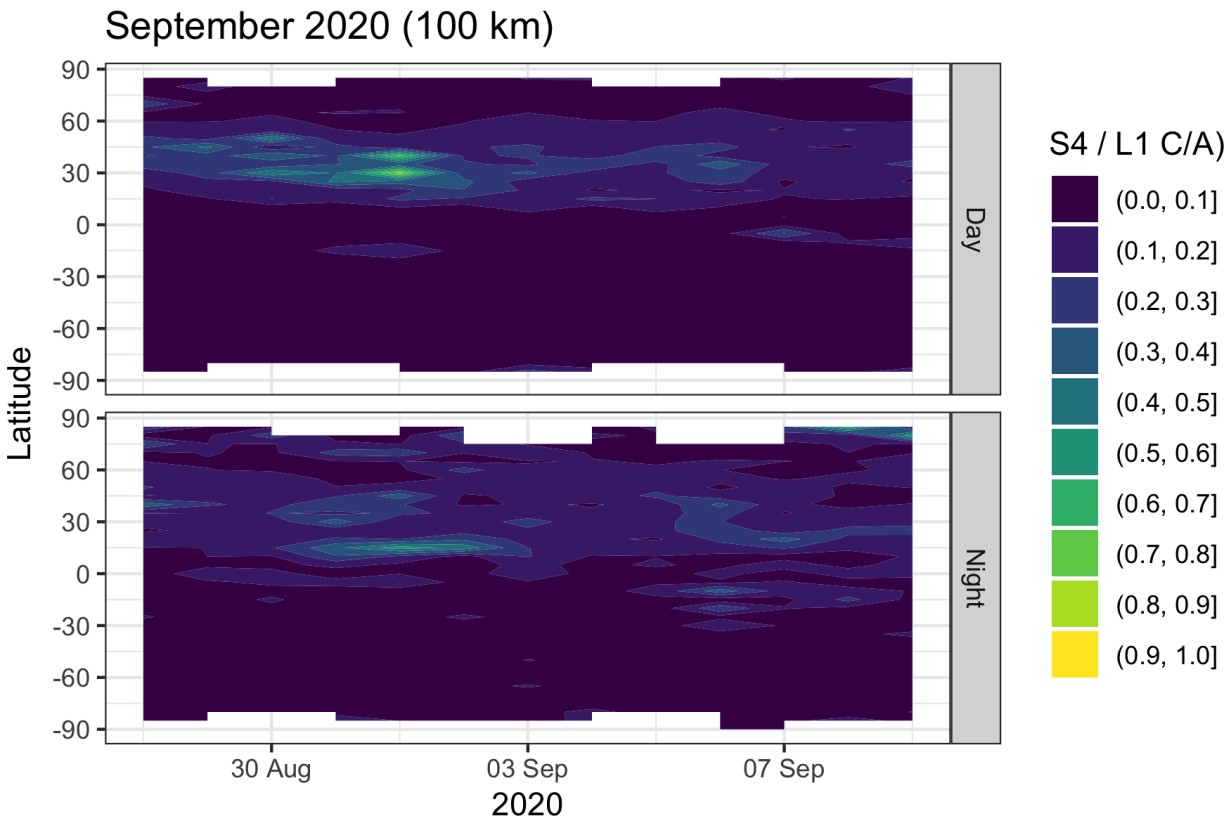

EUMETSAT

Ionospheric monitoring capabilities of the RO instrument on EPS-SG and products description

RO on EPS-SG: Ionospheric monitoring capabilities

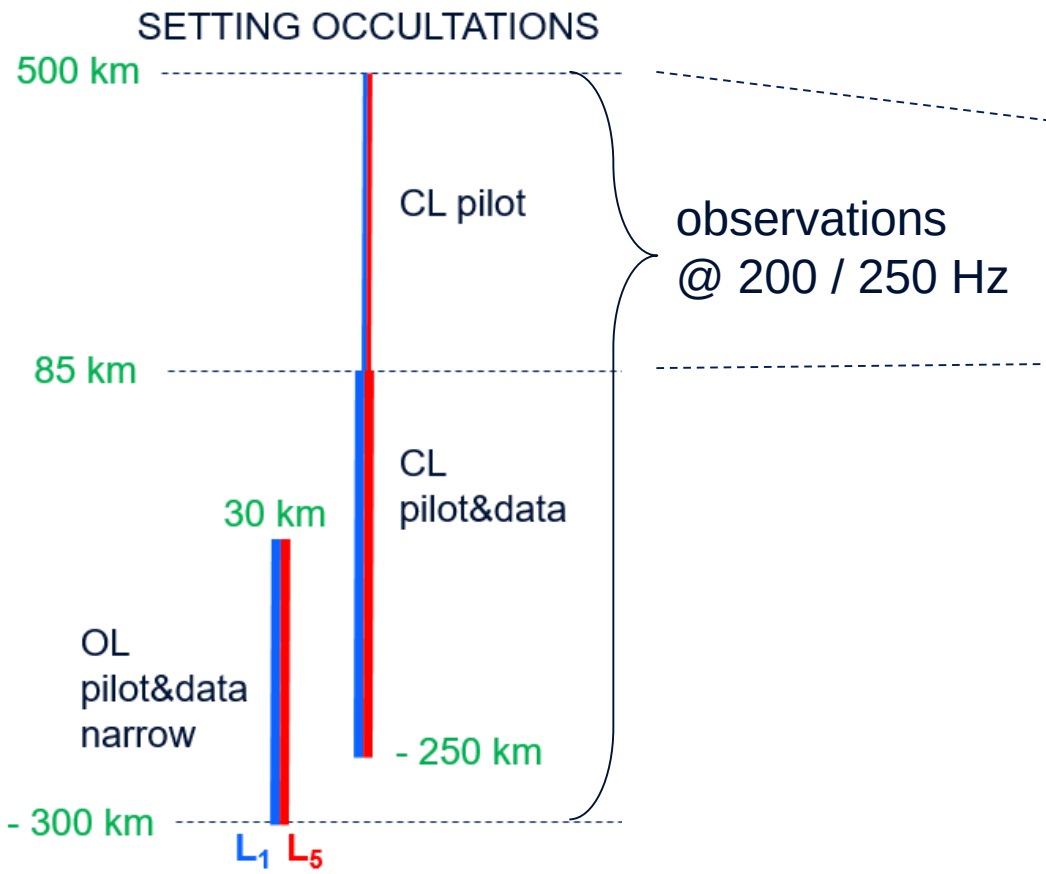

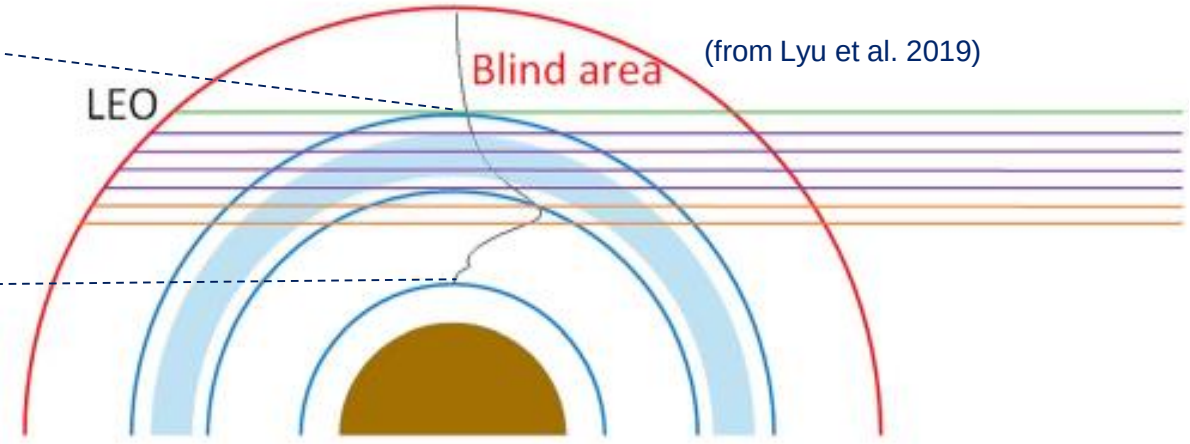

(from Lyu et al. 2019)

Signal	Frequency	Constellation
L1 C/A	1575.42 MHz	GPS
L1C (d, p)	1575.42 MHz	GPS
L5 (I, Q)	1176.45 MHz	GPS
E1 (b, c)	1575.42 MHz	Galileo
E5a (I, Q)	1176.45 MHz	Galileo
B1	1575.42 MHz	Beidou
B2A	1176.45 MHz	Beidou

(see further details on the presentation *RO_Mission_Overview_Products_Data_Access* presentation given on 27/10)

2 rising/setting ionospheric occultation will be contemporaneously available

EUMETSAT

Ionospheric information on L1b RO products

W_XX-EUMETSAT-Darmstadt,SAT,SGA1-RO_-1B-BND_C_EUMT_20211004211813_G_D_20070912120047_20070912120515_T_N_G06.nc

- status
  - satellite
  - instrument
  - processing
- data
  - occultation
  - receiver
    - satellite
    - orbit
    - clock
  - level_1b
  - level_1a
  - ionosphere
  - transmitter
    - satellite
    - orbit
    - clock
  - earth_orientation_parameters
- quality

/status
conveying information about the status of the satellite, the instrument, and the processing chain

/occultation:
georeferencing information for the neutral atmospheric occultation

/receiver; /transmitter

- satellite
  - xyz
  - satellite_in_eclipse
  - antenna_phase_centre
  - antenna_orientation
  - centre_of_mass
- orbit
  - centre_of_mass
  - antenna_phase_centre
- clock
  - t
  - type
  - bias
  - rate
  - utc_abstime
  - utc_absdate

(see further details on the presentation *RO_Mission_Overview_Products_Data_Access* presentation given on 27/10)

EUMETSAT

Ionospheric information on L1b RO products

W_XX-EUMETSAT-Darmstadt,SAT,SGA1-RO_-1B-BND_C_EUMT_20211004211813_G_D_20070912120047_20070912120515_T_N_G06.nc

- status
  - satellite
  - instrument
  - processing
- data
  - occultation
  - receiver
    - satellite
    - orbit
    - clock
  - level_1b
  - level_1a
  - ionosphere
  - transmitter
    - satellite
    - orbit
    - clock
  - earth_orientation_parameters
- quality

/level_1a

- level_1a
  - gps_start_abstime
  - utc_start_absdate
  - utc_start_abstime
  - gps_start_absdate
  - combined
    - L1
    - L5

/L1; /L5

Time series of

- (ex)-phase, SNR, (ex)-pseudorange
- LEO/GNSS positions & velocities interpolated @measurement time stamps
- GNSS azimuth/elevation angles in the RO antenna
- + other information

/level_1b

- Neutral Atmospheric Bending angles profiles

(see further details on the presentation *RO_Mission_Overview_Products_Data_Access* presentation given on 27/10)

EUMETSAT

Ionospheric information on L1b RO products

W_XX-EUMETSAT-Darmstadt,SAT,SGA1-RO_-1B-BND_C_EUMT_20211004211813_G_D_20070912120047_20070912120515_T_N_G06.nc

- status
  - satellite
  - instrument
  - processing
- data
  - occultation
  - receiver
    - satellite
    - orbit
    - clock
  - level_1b
  - level_1a
  - ionosphere
  - transmitter
    - satellite
    - orbit
    - clock
  - earth_orientation_parameters
- quality

- ionosphere
  - gps_start_absdate
  - gps_start_abstime
  - utc_start_abstime
  - utc_start_absdate
  - thinned
  - high_resolution
  - occultation

/occultation

georeferencing information for the ionospheric occultation

/thinned; /high_resolution

The content of these groups is identical, apart from the number of vertical levels.
100 m for high_resolution data
1000 m for thinned data

The two groups contain arrays of

- L1 and L5 bending angles
- impact parameters / impact heights
- L1 and L5 scintillation indexes (S_4, σ_Φ)
- Tangent points geolocation parameters
  - Latitude/Longitude
  - Azimuth toward north

EUMETSAT

L2 ionospheric products

- Will be provided by ROM-SAF (see https://www.romsaf.org)

- Electron density profiles (from ~100 km **to orbit altitude** obtained from dual frequencies carrier phases data)

- Scintillations indices profiles

- Need to develop methods for extending the profile to the LEO orbit (see next slides)

Electron density profile extension to EPS-SG satellites orbit: recent results

EPS-SG ionospheric RO challenge:
The topside “Ne-skeleton”: the simple linear Vary Chapman model

- Olivares-Pulido et al. (2016) demonstrated that:

(1) A linear relationship of the scale height, H, with respect to height, h, is a realistic model for the topside part of the electron density profiles directly derived from GNSS ionospheric radio occultation measurement (variability contemplated at the Vary-Chap model, Nsumei et al., 2012).

(2) Such scale height linear increase with height is consistent with the corresponding linear increase of temperature and the simple first-principles behind the Chapman model.

- This LVC model is able to take into account the change of the scale height in the topside part of the electron density profile, while, at the same time, it retains the mathematical simplicity of the Chapman model.

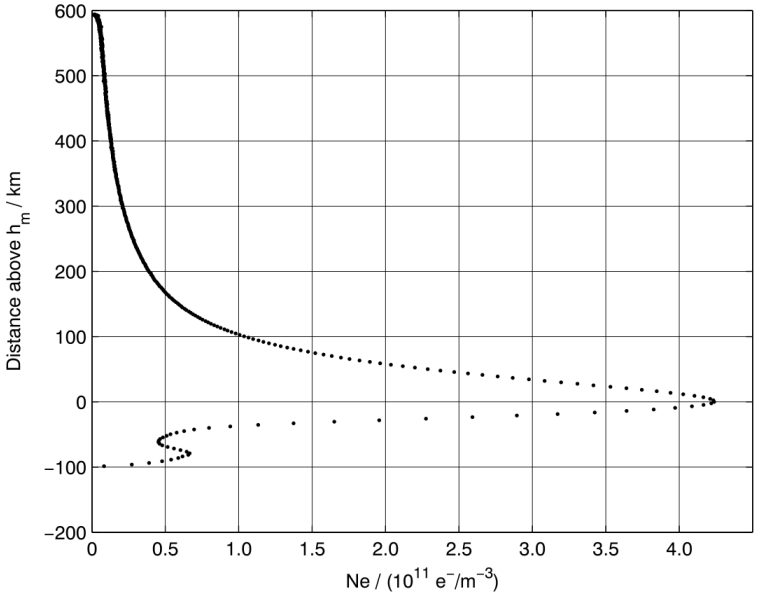

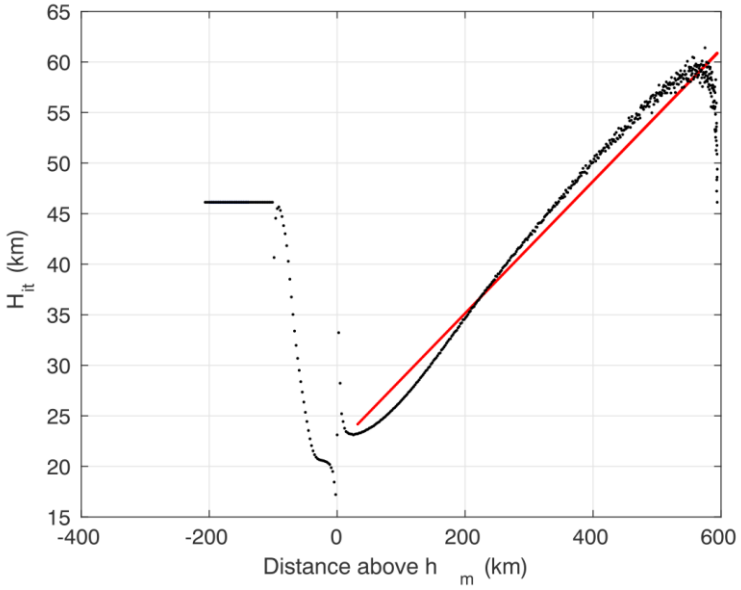

EPS-SG ionospheric RO challenge:
The simple linear Vary Chapman model extrapolates very well

- Hernández-Pajares et al. 2018 showed how LVC enable a new way(accurate and simple) of extrapolating the electron density above the F2 electron density peak: the so called Vary-Chap Extrapolation Technique (VCET):

(1) It was applied to the output of an updated version of the Improved Abel Transform Inversion technique (Hernández-Pajares et al. 2000), to +3000 representative ionospheric radio occultations gathered by COSMIC/FORMOSAT-3 constellation, in solar maximum and minimum conditions, and geomagnetically disturbed conditions.

(2) It is shown that VCET performs much better than other classical Chapman models, with 60% of occultations showing relative extrapolation errors below 20%, in contrast with conventional Chapman model extrapolation approaches with 10% or less of the profiles with relative error below 20%..

EUMETSAT

EPS-SG ionospheric RO challenge:
One solution: Abel Vary-Chap Hibrid Ionospheric RO model (AVHIRO)

- Lyu et al. (2019) summarized the definition and validation of two new strategies, to invert incomplete GNSS RO ionospheric measurements, such as the future EPS-SG (RO measurements with impact parameter much from 500 km down from below the LEO height of ~817 km):

(1) The AVHIRO, based on simple First Principles, very precise in general (an update is ongoing), and well-suited for post-processing.

(2) The Simple Estimation of Electron density profiles from topside Incomplete RO data (SEEIRO), is less precise but yields very fast estimations, suitable for Near Real-Time (NRT) determination.

- First versions of both techniques were assessed with a set of 546 representative COSMIC/FORMOSAT-3 ROs, with relative errors of 7% and 11% for AVHIRO and SEEIRO respectively.

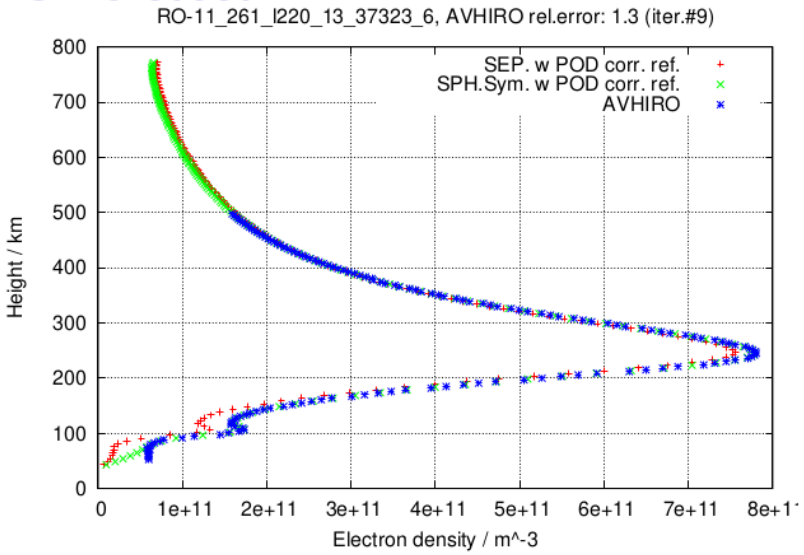

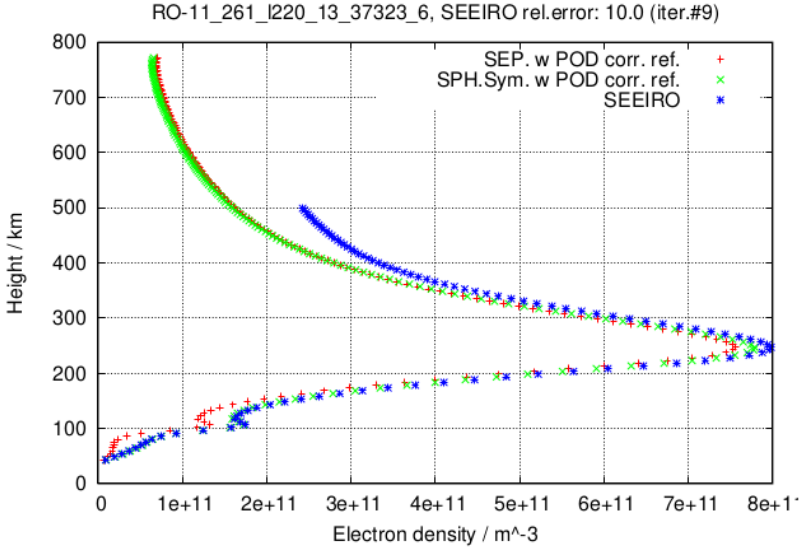

EUMETSAT

1D-Var retrieval of Electron Density profiles

- A new one-dimensional variational (1D-Var) retrieval approach has been developed by ROM-SAF (Sean Healy, *ECMWF* and Ian Culverwell, *MetOffice*) in which
  - truncated RO measurements are accounted for as part as of a forward operator H(**x**)
  - which maps **Ne(h)** to the observation space (the $\boldsymbol{\alpha_{L5}(a) - \alpha_{L1}(a)}$ bending angle difference, a is the impact parameter)
  - by assuming that Ne(h) can be modelled as the sum of (several) one-dimensional Chapman layers, each one modelled by 4 parameters (defining the state vector **x**)
    - electron density peak and it's height
    - scale height and it's gradient

EUMETSAT

1D-Var retrieval of Electron Density profiles

- Aim of the 1D-Var retrieval approach is to combine the a priori information in the state vector ($\mathbf{x_b}$) with a vector of observations ($\mathbf{y}$) in a statistically optimal way (Rodgers 2000).

- It involves minimising a cost function of the form:

$$J(\mathbf{x}) = \frac{1}{2}(\mathbf{x}-\mathbf{x_b})^{\mathbf{T}}\mathbf{B}^{-1}(\mathbf{x}-\mathbf{x_b}) + \frac{1}{2}(\mathbf{y}-H(\mathbf{x}))^{\mathbf{T}}\mathbf{R}^{-1}(\mathbf{y}-H(\mathbf{x}))$$

  B: assumed background error covariance matrix
  R: observation error covariance matrix

- The 1D-Var adjusts the Chapman layer parameters (4 per each layer) to fit the $\alpha_{L5}(a) - \alpha_{L1}(a)$ difference, and this naturally provides a new estimate of the ionosphere also above 500 km.

EUMETSAT

1D-Var retrieval of Electron Density profiles

GRAS_1B_M02_20200801185254Z_20200801185816Z_N_T_20210507160605Z_G02_NN

- Fit to a single Chapman layer
- Assimilating L_2-L_1 bending angles from 200 to 500 km

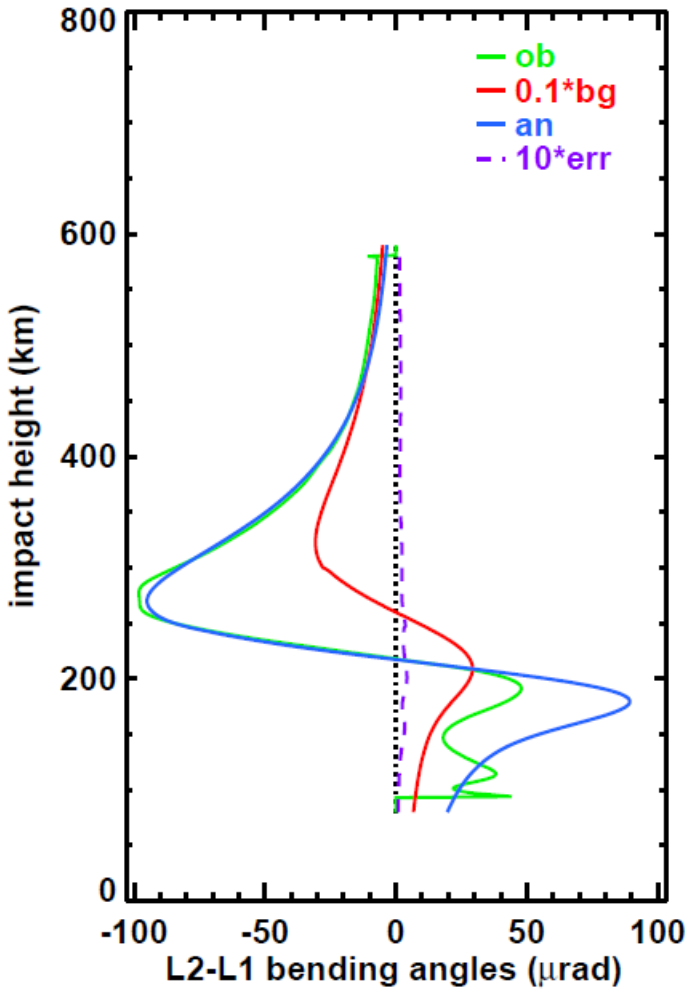

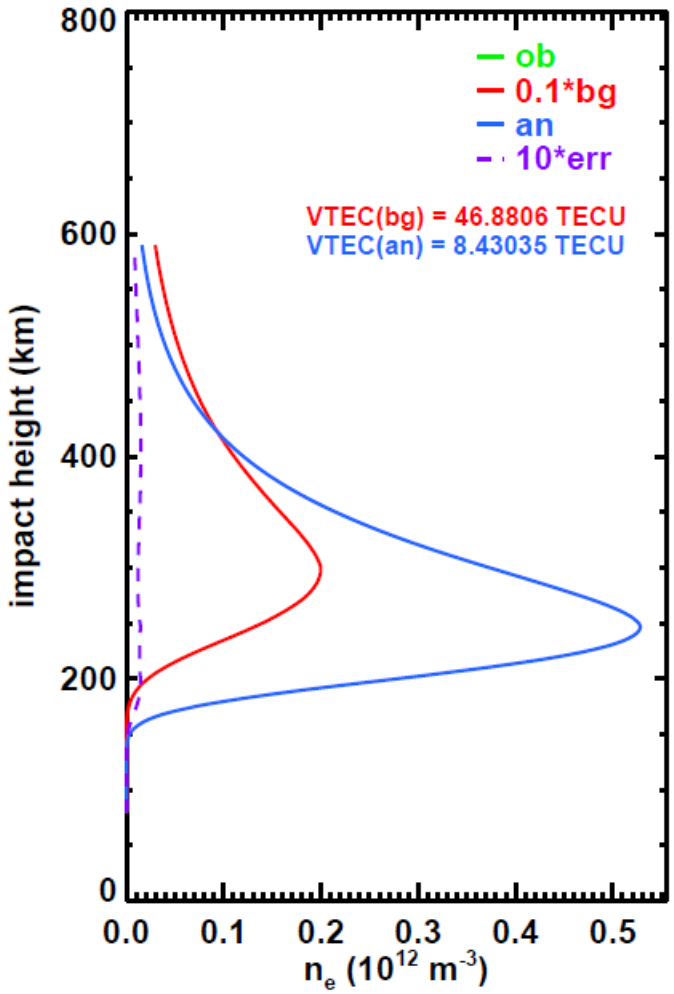

EUMETSAT

1D-Var retrieval of Electron Density profiles

GRAS_1B_M02_20200801185254Z_20200801185816Z_N_T_20210507160605Z_G02_NN

- Fit to double Chapman layers
- Assimilating L_2-L_1 bending angles from 120 to 500 km

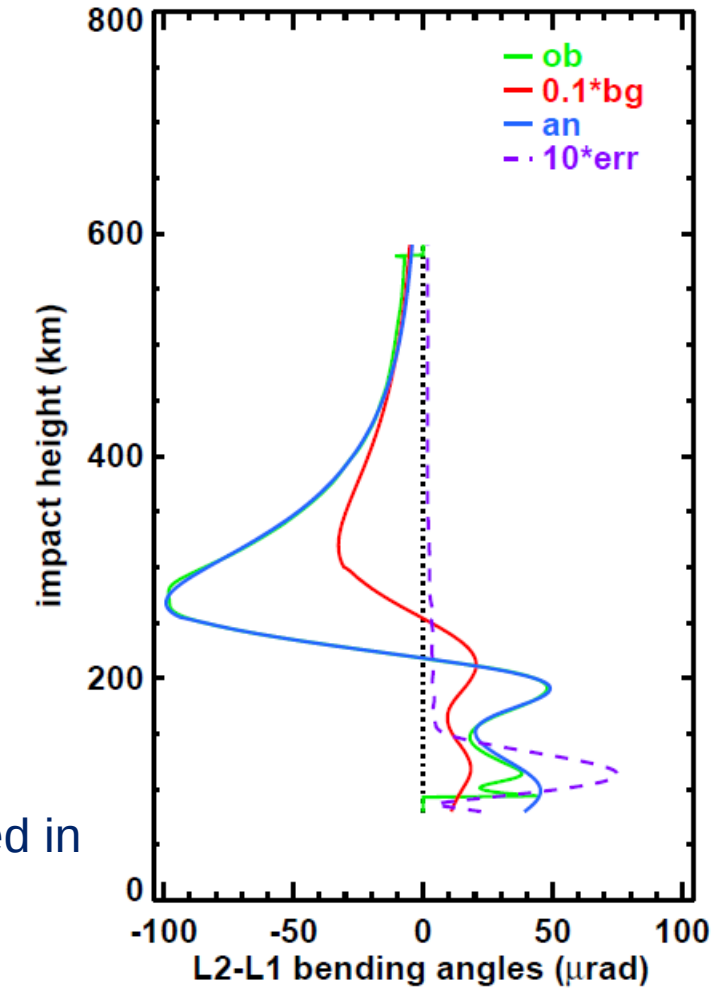

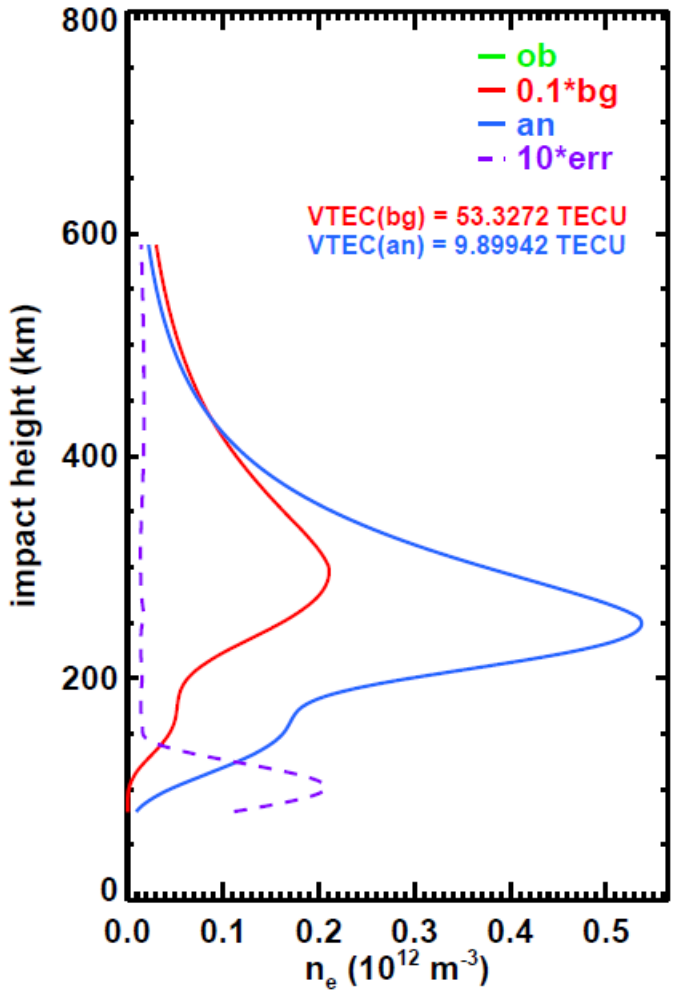

All the details have been just published in the following ROM-SAF Report: https://www.romsaf.org/general-documents/rsr/rsr_42.pdf

EUMETSAT

Summary

- Ionospheric Monitoring and Space Weather applications using Radio Occultation observations
- Ionospheric capabilities of Radio Occultation instruments on board EPS and EPS-SG missions
- Ionospheric product that will be made available for EPS-SG
- Electron Density product extension to LEO orbit for truncated Radio Occultation ionospheric measurements: current developments

MTG + EPS-SG

EUMETSAT

FUTURE FOCUS

Weather and climate data like never before

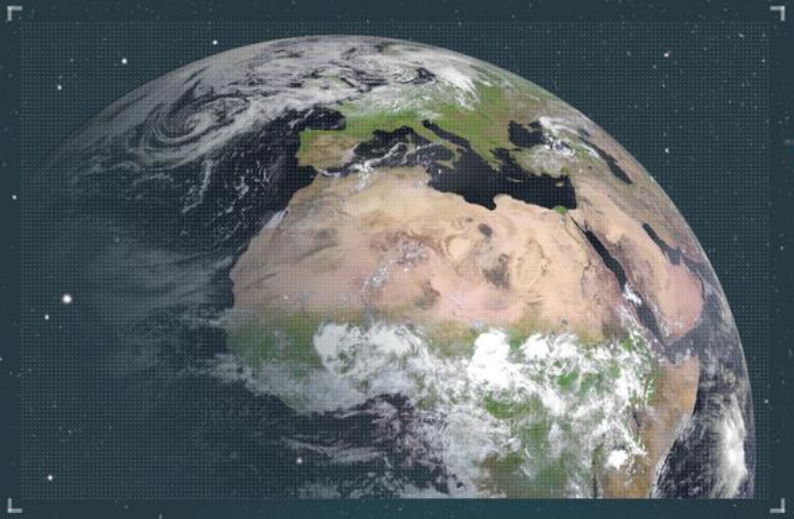

EPS-SG Radio Occultation Mission Overview, Products and Data Access

Thank you!